RESEARCH MEMORANDUM

A TRANSONIC WIND-TUNNEL INVESTIGATION OF THE EFFECTS OF BODY INDENTATION, AS SPECIFIED BY THE TRANSONIC DRAG-RISE RULE, ON THE AERODYNAMIC CHARACTERISTICS AND FLOW PHENOMENA OF A 45° SWEPTBACK-WING—BODY COMBINATION

By Harold L. Robinson

Langley Aeronautical Laboratory
Langley Field, Va.

NATIONAL ADVISORY COMMITTEE
FOR AERONAUTICS

WASHINGTON

February 9, 1953

1W

NATIONAL ADVISORY COMMITTEE FOR AERONAUTICS

RESEARCH MEMORANDUM

A TRANSONIC WIND-TUNNEL INVESTIGATION OF THE EFFECTS OF BODY INDENTATION, AS SPECIFIED BY THE TRANSONIC DRAG-RISE RULE, ON THE AERODYNAMIC CHARACTERISTICS AND FLOW PHENOMENA OF A 45° SWEPTBACK-WING–BODY COMBINATION

By Harold L. Robinson

SUMMARY

The aerodynamic characteristics and flow phenomena at transonic speeds for a 45° sweptback wing mounted alternatively on a cylindrical body and an indented body are compared herein. The first of these wing-body combinations had a body which was cylindrical at the wing stations; whereas, the body of the second configuration was indented at the wing stations so that the axial distribution of the cross-sectional areas, normal to the fuselage center line, of the wing-body combination was the same as that of the first body alone. The indented body was designed in accordance with Whitcomb's transonic drag-rise rule given in NACA RM L52H08.

Indentation eliminated the zero-lift drag rise associated with the wing at a Mach number of 1. The drag of the wing-body combination at transonic speeds for lift coefficients up to 0.4 has been reduced by body indentation by approximately the same amount as at zero lift. Flow studies indicated that the elimination of the drag rise associated with the wing near the speed of sound by body indentation was primarily caused by a marked reduction in strength of the shock field.

INTRODUCTION

An interpretation of transonic zero-lift drag-rise characteristics of wing-body configurations is presented in reference 1. Whitcomb in reference 1 introduces a concept (to be called the transonic drag-rise rule) by which the drag rise is indicated to be primarily dependent on the axial development of the cross-sectional area normal to the air

stream. It was also shown that a 45° sweptback-wing–body combination, with the body indented so that the configuration had the same axial area distribution as the original body alone, exhibited essentially the same zero-lift drag rise near the speed of sound as the body alone.

The results of an extended investigation of the 45° sweptback wing mounted alternatively on the cylindrical and indented bodies are presented in the present report. The objectives of these tests were to evaluate the effects of the body indentation on the aerodynamic characteristics of the configurations for the lifting conditions, to ascertain the flow phenomena responsible for the reduction in the transonic drag rise, and, finally, to provide information that might lead to further reductions of the drag rise by additional modifications of the wing-body combination.

The tests reported herein were made at Mach numbers of 0.80 to 1.10 and at angles of attack from 0° to 12°. Reynolds numbers for this investigation, based on the mean aerodynamic chord of 6.125 inches, varied from 1.8×10^6 to 2.10×10^6. A similar investigation of a zero-taper-ratio, unswept-wing–body combination is reported in reference 2.

APPARATUS AND METHODS

Tunnel

The investigation was performed in the Langley 8-foot transonic tunnel, which has a dodecagonal slotted test section and is capable of continuously variable operation through the speed range up to a Mach number of approximately 1.13. Detailed discussions of the design and calibration of this tunnel are presented in references 3 and 4.

Tunnel-wall-interference corrections are not required for the data presented in this report. Choking and blockage effects for the slotted test section, especially for the relatively small model to tunnel size, are negligible. Effects of wall-reflected disturbances on the drag results, as discussed in reference 4, have been practically eliminated for the data presented herein by offsetting the model from the tunnel center line and by adjusting the data to the condition of free-stream static pressure at the base of the model.

Models

The steel wing employed for this investigation incorporated the NACA 65A006 section parallel to the air stream, a sweepback angle of the quarter chord line of 45°, a taper ratio of 0.6, and an aspect ratio of 4.

This wing, as shown in figure 1, was mounted alternatively on one of two bodies. The first body was cylindrical at the wing location, while the second body was indented at the wing location. The indentation was designed so that the area removed from the body at each longitudinal station was equal to the exposed wing cross-sectional area at the same station (after indentation) normal to the air stream. Radii of the bodies are presented in table I and axial variations of the cross-sectional areas of the configurations are presented in figure 2.

The models were sting-mounted in the tunnel, the diameter of the sting at the base of the model being 3.12 inches compared with 3.75 inches for the body.

Measurements

Lift, drag, and pitching moment.- The normal, axial, and pitching-moment characteristics of the models were measured by an internally mounted electrical strain-gage force balance. An estimate of the maximum errors is given in the following table:

Mach number	C_L	C_D	C_m
0.60	0.016	0.002	0.003
1.00	0.008	0.001	0.002

The errors are usually less than these maximum values.

Angle of attack.- The angle of attack was measured by an electrical strain gage mounted in the nose of the model. A more complete description of the angle-of-attack measuring system is given in reference 2, and, as reported therein, the measurements of angle of attack are believed to be accurate to within $\pm 0.1^\circ$.

Flow surveys.- The schlieren photographs presented in this report were obtained with the same apparatus used to obtain the schlieren photographs of references 1 and 2; this apparatus is fully described in reference 4. The center of the field of view for the schlieren photographs is on the tunnel center line. The model was displaced below the center line for the side-view photographs which were obtained simultaneously with the force data. For the plan-view photographs, the model was rotated and displaced so that the wings were vertical and a wing tip was in the schlieren field. A sketch showing the relative location of the model and the orifices used to measure pressures on the tunnel wall is shown

in the lower right-hand corner of the flow-survey composites for 0° angle of attack (fig. 10). The accuracy of the free-stream Mach numbers presented herein is within 0.005; however, it is believed that the wall Mach numbers presented are more accurate than this amount.

PRESENTATION OF RESULTS

Lift, Drag, and Pitching Moment

The basic aerodynamic coefficients for the wing-body combinations for various free-stream Mach numbers are presented in figure 3 in the form of angle of attack, pitching-moment coefficient, and drag coefficient plotted against lift coefficient. The coefficients are based on the total wing area of 1 square foot. This area includes that enclosed by the body. Pitching-moment coefficients are referred to the quarter chord of the wing mean aerodynamic chord of 6.125 inches. All the coefficients have been adjusted to the condition of free-stream pressure at the base of the model. The drag coefficients of the wing with body interference, presented in figure 4, resulted from subtraction of the lift and drag coefficients for the cylindrical body alone, obtained from reference 2, from those for the wing-body combinations. The variation of drag coefficient with Mach number presented in figures 5 and 6 for the wing-body combinations and the wing with interference was obtained from cross-plotting figures 3(c) and 4, respectively. The maximum lift-drag ratios and the lift coefficients for maximum lift-drag ratio, (fig 7) were also obtained from figures 3(c) and 4. The center-of-pressure locations, presented in figure 8, were computed by the standard relation

$$x_{cp} = \left(0.25 - \frac{C_m}{C_L}\right)100$$

A comparison of various aerodynamic characteristics for a level flight condition is presented in figure 9.

Flow Surveys

Tunnel-wall Mach number distributions and accompanying schlieren photographs for the zero-lift case are presented in figure 10. The drawings of the models are to the same scale as the photographs. The wall Mach number distributions presented were obtained simultaneously with the plan-view photographs shown in the figure. In this figure the distance from the model center line to the mean value of the free-stream Mach number represents (to scale) the distance from the model center line to the orifices in the tunnel-wall panels. The sketches near the lower right-hand corner of figure 10 further represent the relative location of the model to the Mach number survey panels. As an aid to comparison,

data presented on the left-hand pages of figure 10 are for the wing cylindrical-body combinations while the data on the corresponding facing pages are for the indented-body combinations at the same Mach number.

The schlieren fields for the lifting case, presented in figure 11, are oriented with respect to the configuration as indicated by the bottom schlieren photographs and configuration outlines.

DISCUSSION OF RESULTS

Force Characteristics

Drag.- For the sweptback wing, as shown in reference 1, the drag rise of the wing with interference at zero lift and Mach number of 1, the design condition, has been essentially eliminated by body indentation and has been delayed to a Mach number of 1.05 (fig. 6). At a Mach number of 1 and at lift coefficients to 0.4, the drag reduction for the lifting case due to body indentation is the same as that at zero lift; however, as the lift coefficient is increased above 0.4 and the Mach number is increased beyond 1, the effect of the indentation is reduced (fig. 5).

At subsonic velocities, the drag for zero lift has been reduced by body indentation; however, at lift coefficients above 0.2, body indentation increased the drag at subsonic Mach numbers (figs. 3(c) and 5).

While body indentation eliminated the drag rise at sonic velocities and at low lift coefficients for the swept wing reported herein, body indentation did not eliminate this drag rise for the unswept wing with zero taper ratio of reference 2. It is believed that the shock associated with the forward region of the indentation for the unswept-wing–body combination probably caused a local thickening or separation of the boundary layer which resulted in an effective decrease in the depth of the indentation. These factors caused departures from the ideal cross-sectional area distribution given by a simple consideration of only the geometrical areas of the configuration and, thus, had adverse effects on the induced velocities in the flow field of the wing. The indentation for the swept wing was more gradual than that for the unswept wing; accordingly, the adverse separation effects were not as severe for the swept wing. Therefore, the indentation with the swept wing was more effective in reducing the drag rise than that for the unswept wing.

Maximum lift-to-drag ratios.- As a consequence of the large drag reductions at lifting conditions and at transonic speeds, the maximum lift-to-drag ratios of the indented wing-body configuration was higher than that for the corresponding cylindrical configuration (fig. 7). In general, the greatest maximum lift-to-drag ratio difference occurred near

a Mach number of one. The difference in maximum lift-to-drag ratio was reduced as the Mach number was increased beyond 1. There was a tendency for the maximum lift-to-drag ratios to occur at lower values of the lift coefficient for the indented configuration where the lift-to-drag ratio was increased by body indentation.

If the drag level of a wing-body combination were lower than that of the configuration employed for these tests, the increase in maximum lift-to-drag ratio due to indentation would be greater than that shown in figure 7(a). The comparison shown in figure 7(b) represents an extreme case applying to a hypothetical fuselage having extremely low drag. At this condition, the maximum lift-to-drag ratio for the case of the wing with cylindrical body interference at a Mach number of 1 was 11.2, while that for the comparable indented case was 16.0.

Pitching moment.- Examination of the pitching-moment data (fig. 3(b)) indicates that, for Mach numbers between 0.90 to 1.03, the lift coefficient where $\partial C_m/\partial C_L$ changes from negative to positive is increased by approximately 0.05 by indenting the body. This effect is not important enough to alter aircraft designs but it is interesting to note that body shape has an effect on the stability characteristics usually associated with wing-tip phenomena.

For lift coefficients up to 0.6, the center of pressure was more forward for the indented case at all Mach numbers except at the highest Mach number investigated (fig. 8). At a lift coefficient of 0.2, the Mach number at which large rearward movement of the center of pressure with Mach number is first evident is 0.05 higher for the indented wing-body combination than for the cylindrical wing-body combination; however, forward center-of-pressure shifts with increasing Mach number above 1 are noted for the cylindrical configuration, while the indented configuration continues to exhibit a rearward shift.

For the unswept wing investigated in reference 2, body indentation had no appreciable effect on the longitudinal center-of-pressure location. It is concluded, therefore, that indenting the body caused the center of pressure to move inboard which, for the swept wing reported herein, was tantamount to a forward movement of the center of pressure.

Lift.- Reference to figure 3(a) indicates that body indentation had little effect on the lift characteristics of the two configurations reported herein.

Level-Flight Characteristics

The comparison of the aerodynamic characteristics for a level-flight condition (fig. 9) indicates that above a Mach number of 0.925 the drag

of an airplane incorporating fuselage indentation would be less than one having an unindented fuselage. The large trim changes associated with transonic airplane configurations would be delayed to a Mach number approximately 0.06 higher by body indentation. The forward movement of center of pressure for the cylindrical wing-body combination above a Mach number of 1.02 does not occur for the indented configuration.

Flow Phenomena

As pointed out in reference 1, because of the essential invariance of the stream tube areas with velocity near a Mach number of 1, the flow field about any configuration is relatively extensive. As a result, the greater part of the energy loss for a configuration is due to the large areas of significantly strong shocks outside the local flow regions about the configuration. Accordingly, the wall Mach number distributions presented in figure 10 are an approximate measure of the strength of the shock system about the configuration. The wall Mach number distributions of figure 10 show that, for the transonic Mach numbers, indentation substantially reduced the induced velocities at a distance from the model. The shock strength about the indented wing-body combination has therefore been reduced. The drag reductions shown are associated with these reductions of shock losses. The reduction of the induced velocities is associated with the more gradual area development of the indented-body configuration.

As may be seen in the schlieren photographs and by the Mach number distributions in figure 10, a shock exists behind the wing trailing edge for the cylindrical body combination at Mach numbers of 0.98 and greater. Near sonic velocities this shock is eliminated by body indentation but is still present for the indented body at the highest Mach number investigated.

For the lifting case (fig. 11), the shock originating at the trailing edge of the wing-root–body juncture has been eliminated or greatly reduced in strength (fig. 11(a)). However, the shocks near the wing tip have not been much affected by body indentation (fig. 11(b)). It should be possible to improve further the drag characteristics of a wing-body combination by washing out the wing tips and thus reducing the induced velocities near the tip.

CONCLUSIONS

Analysis of results obtained from a transonic wind-tunnel investigation of a 45° sweptback wing mounted alternatively on an indented

(designed in accordance with the transonic drag-rise rule) and cylindrical body indicate the following conclusions:

1. Body indentation eliminated the zero-lift drag rise associated with the wing at a Mach number of 1 and delayed this drag rise to a Mach number of 1.05.

2. The drag of the wing-body combination at transonic speeds for lift coefficients up to 0.4 has been reduced by body indentation by approximately the same amount as at zero lift. The drag difference between indented and unindented configurations for lifting conditions becomes less as the lift coefficient is further increased or as the Mach number is increased beyond 1. The drag reductions resulted in significant increases of the lift-to-drag ratio at transonic speeds.

3. The lift characteristics of the combinations were little affected by indentation.

4. The center of pressure for lift coefficients below 0.6 is more forward for the indented configuration except for the highest Mach number investigated (1.10) where the reverse is true.

5. Flow surveys indicated that the essential elimination of the drag rise associated with the wing near the speed of sound by body indentation was caused, primarily, by a marked reduction in the strength of the shock field.

Langley Aeronautical Laboratory,
National Advisory Committee for Aeronautics,
Langley Field, Va.

REFERENCES

1. Whitcomb, Richard T.: A Study of the Zero-Lift Drag-Rise Characteristics of Wing-Body Combinations Near the Speed of Sound. NACA RM L52H08, 1952.

2. Williams, Claude V.: A Transonic Wind-Tunnel Investigation of the Effects of Body Indentation, as Specified by the Transonic Drag-Rise Rule, on the Aerodynamic Characteristics and Flow Phenomena of an Unswept-Wing–Body Combination. NACA RM L52L23, 1953.

3. Wright, Ray H., and Ritchie, Virgil S.: Characteristics of a Transonic Test Section With Various Slot Shapes in the Langley 8-Foot High-Speed Tunnel. NACA RM L51H10, 1951.

4. Ritchie, Virgil S., and Pearson, Albin O.: Calibration of the Slotted Test Section of the Langley 8-Foot Transonic Tunnel and Preliminary Experimental Investigation of Boundary-Reflected Disturbances. NACA RM L51K14, 1952.

[redacted]

TABLE I.- FUSELAGE ORDINATES

Station, in.	Radius, in.	
	Cylindrical body	Indented body
0	0	0
.225	.104	.104
.338	.134	.134
.563	.193	.193
1.125	.325	.325
2.250	.542	.542
3.375	.762	.762
4.500	.887	.887
6.750	1.167	1.167
9.000	1.391	1.391
11.250	1.559	1.559
13.500	1.683	1.683
15.750	1.770	1.770
18.000	1.828	1.828
20.250	1.864	1.864
22.500	1.875	1.875
23.125	1.875	1.875
24.125	1.875	1.842
25.125	1.875	1.787
26.125	1.875	1.710
27.125	1.875	1.641
28.125	1.875	1.592
29.125	1.875	1.560
30.125	1.875	1.572
31.125	1.875	1.611
32.125	1.875	1.640
33.125	1.875	1.656
34.125	1.875	1.688
35.125	1.875	1.740
36.125	1.875	1.802
37.125	1.875	1.850
38.125	1.875	1.874
38.375	1.875	1.875
43.000	1.875	1.875

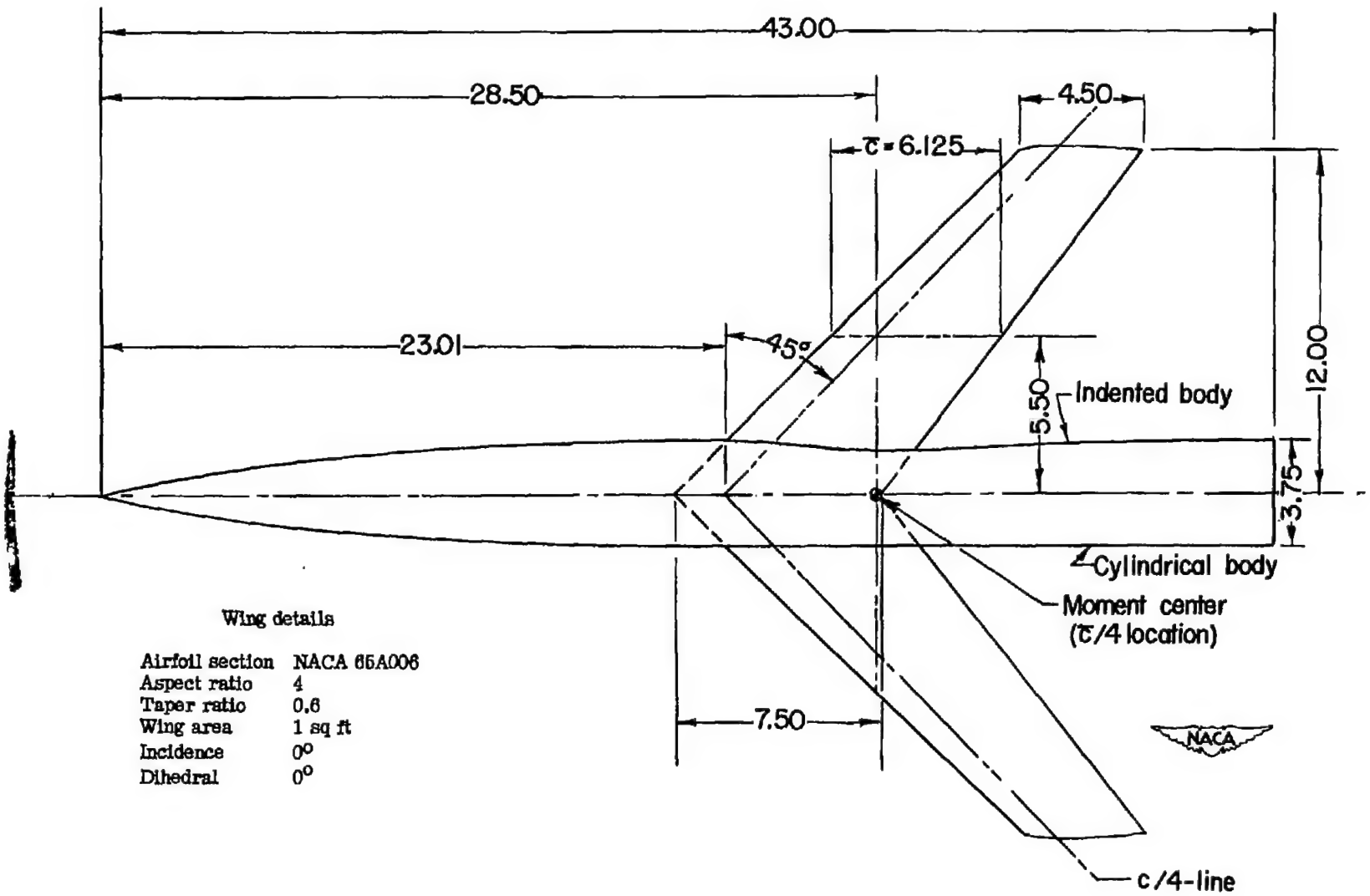

Wing details

Airfoil section	NACA 65A006
Aspect ratio	4
Taper ratio	0.6
Wing area	1 sq ft
Incidence	0°
Dihedral	0°

Figure 1.- Model details. All dimensions in inches.

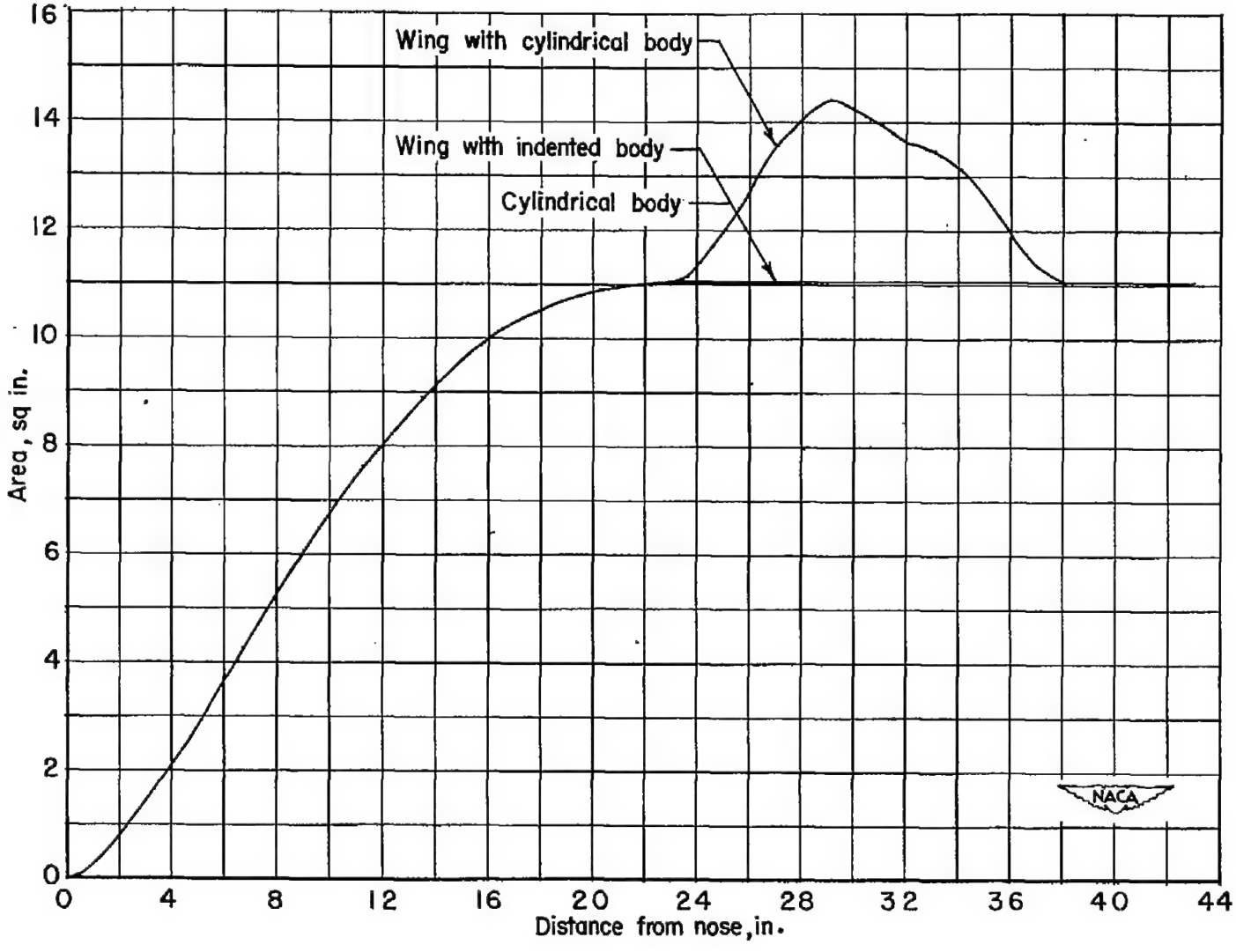

Figure 2.- Cross-sectional areas of models.

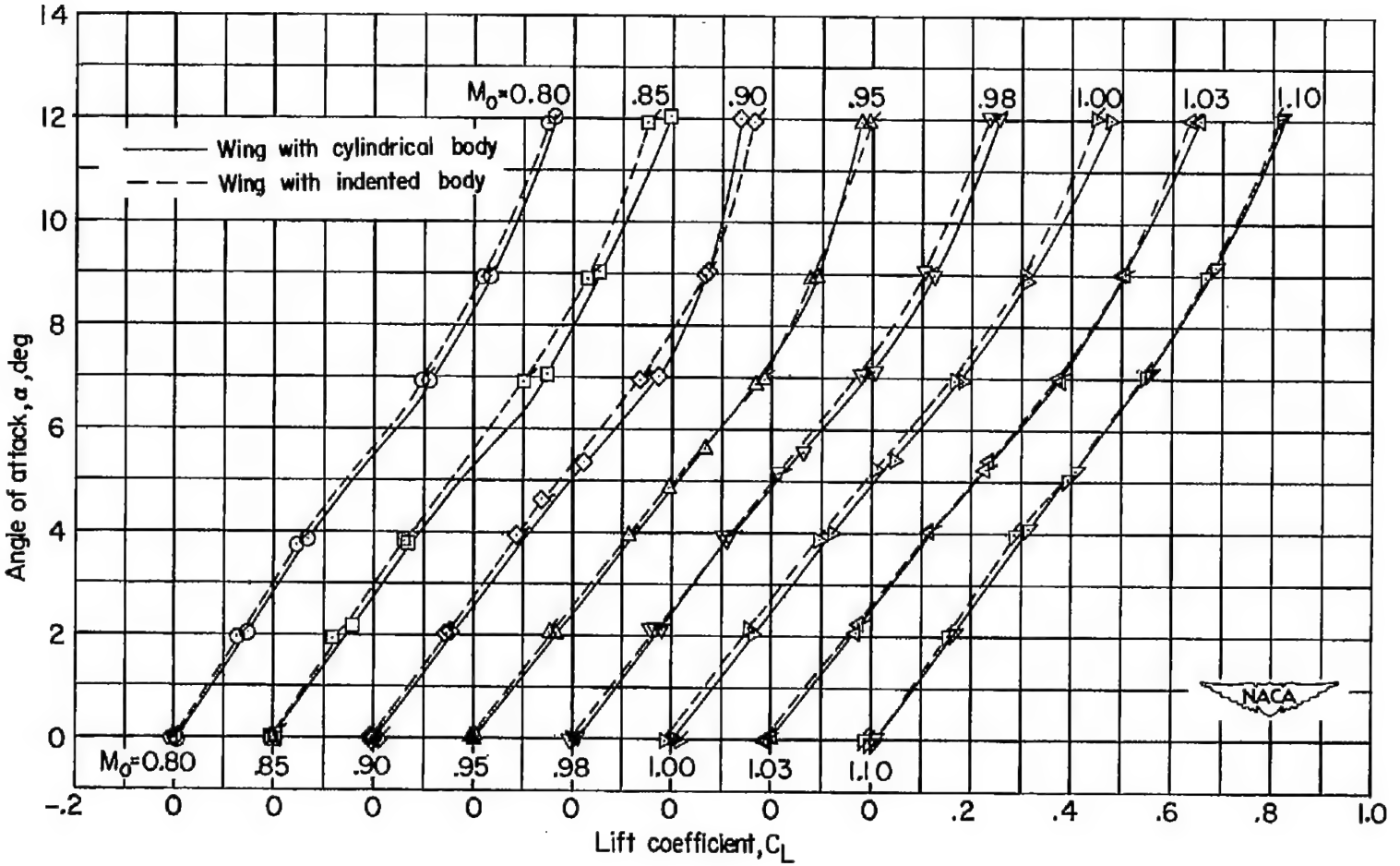

(a) Angle of attack.

Figure 3.- Variation of the basic aerodynamic coefficients with lift coefficient. Wing and body combination. (Flagged symbols indicate wing with indented body.)

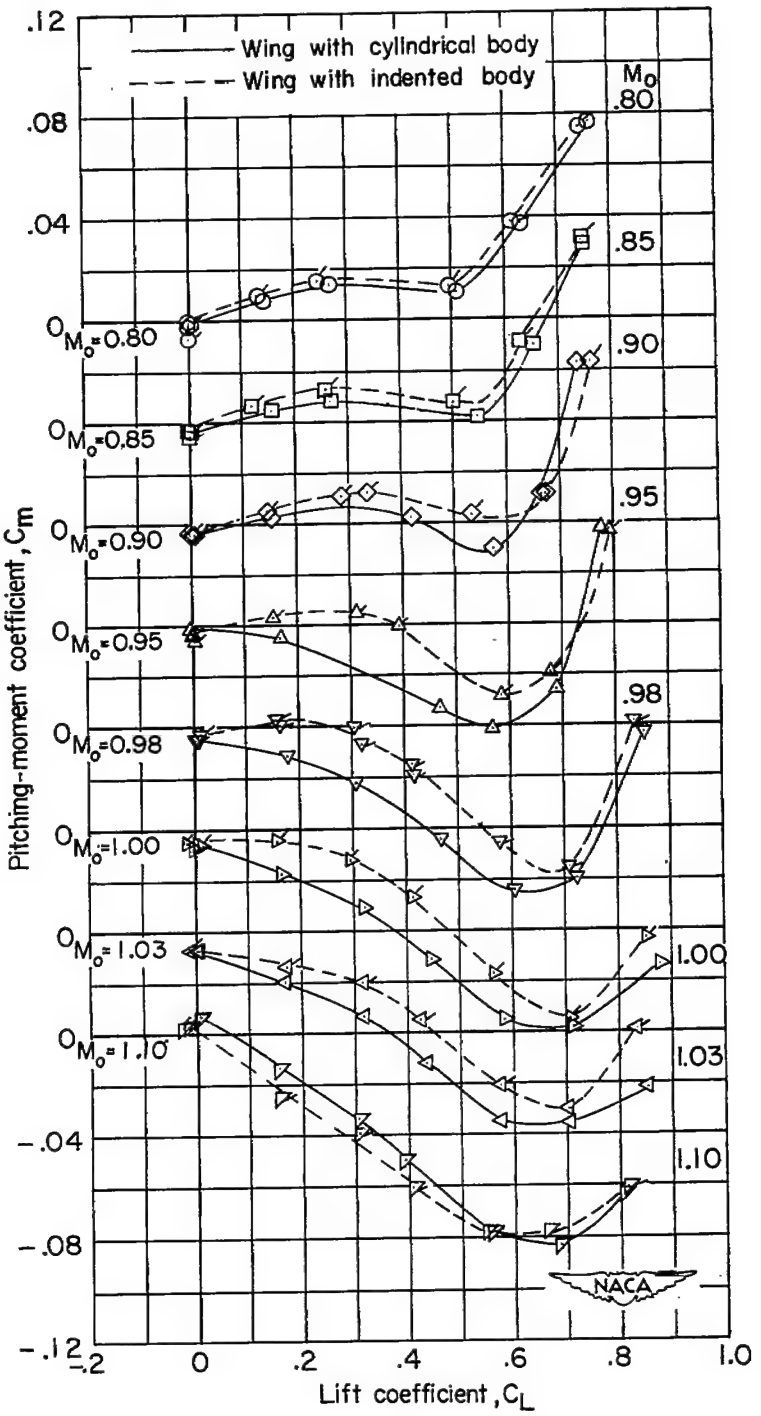

(b) Pitching-moment coefficient.

Figure 3.- Continued.

[redacted]

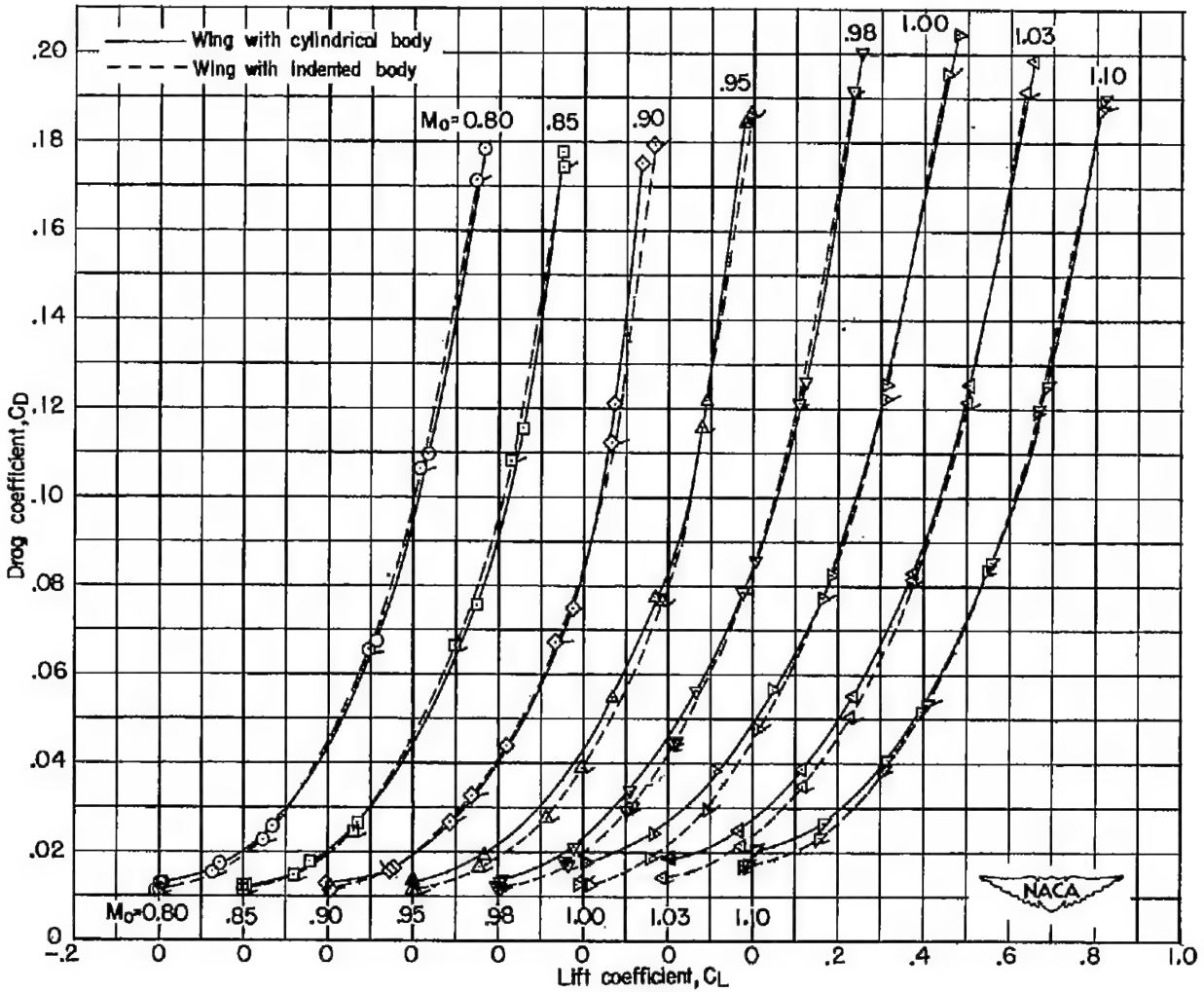

(c) Drag coefficient.

Figure 3.- Concluded.

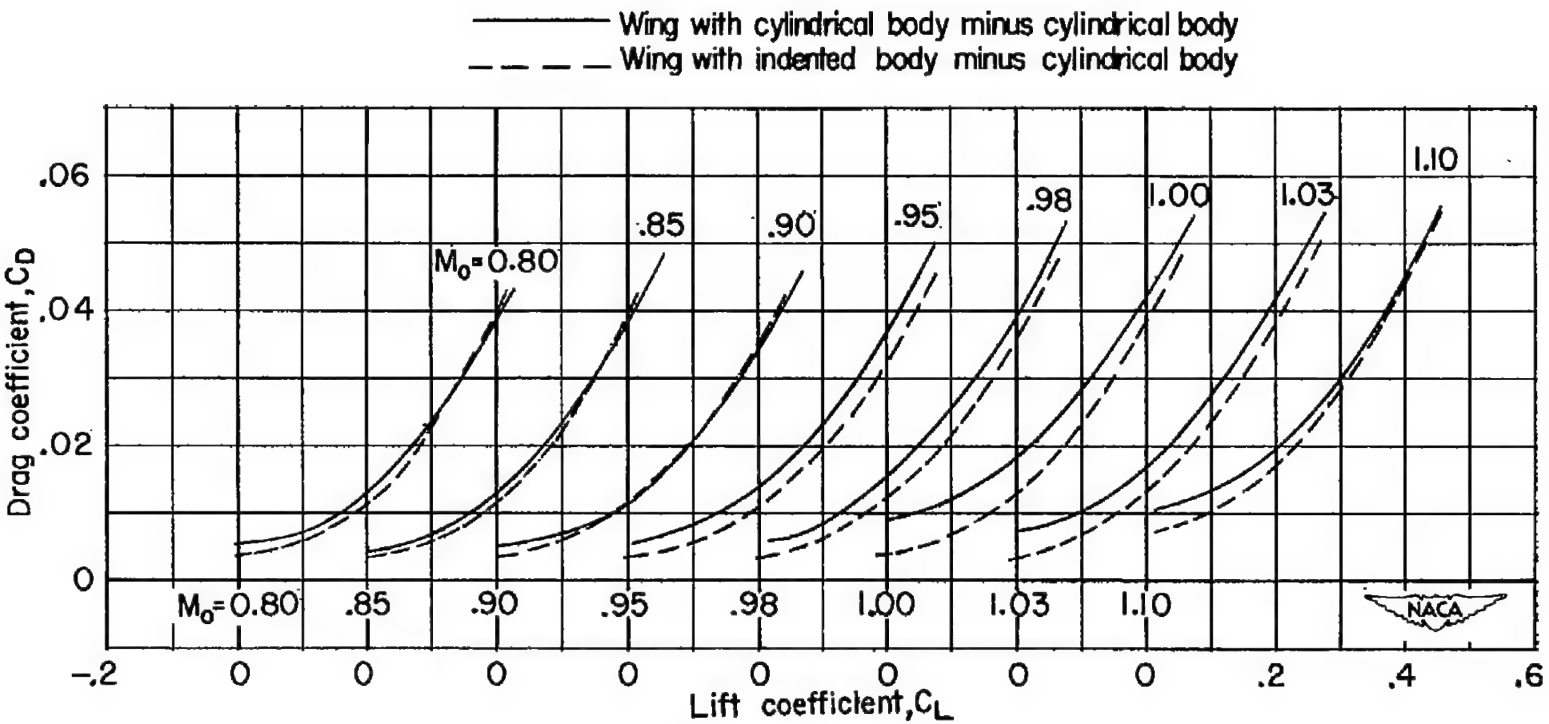

Figure 4.- Variation of drag coefficient with lift coefficient. Wing with interference.

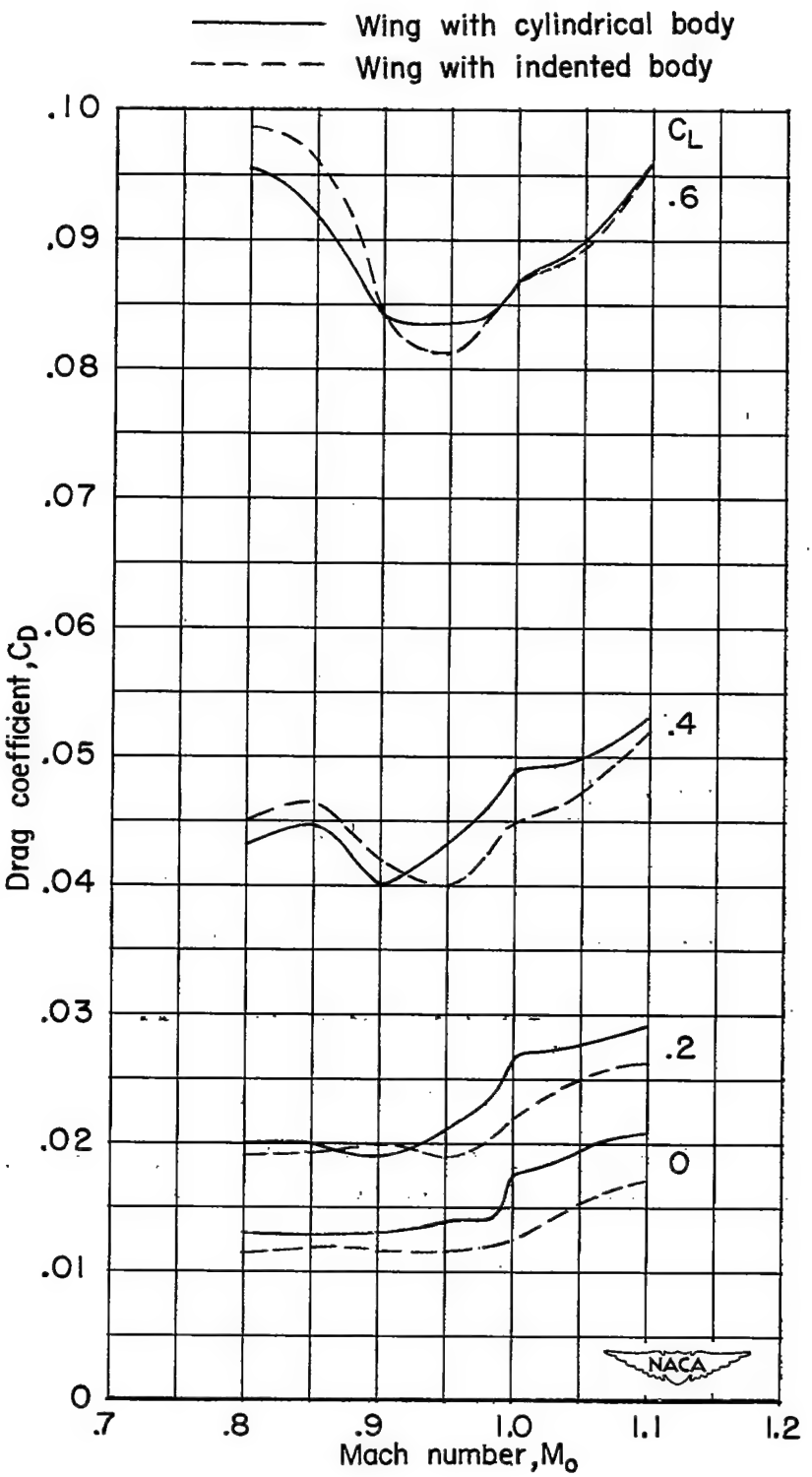

Figure 5.- Variation of drag coefficient with Mach number. Wing with body.

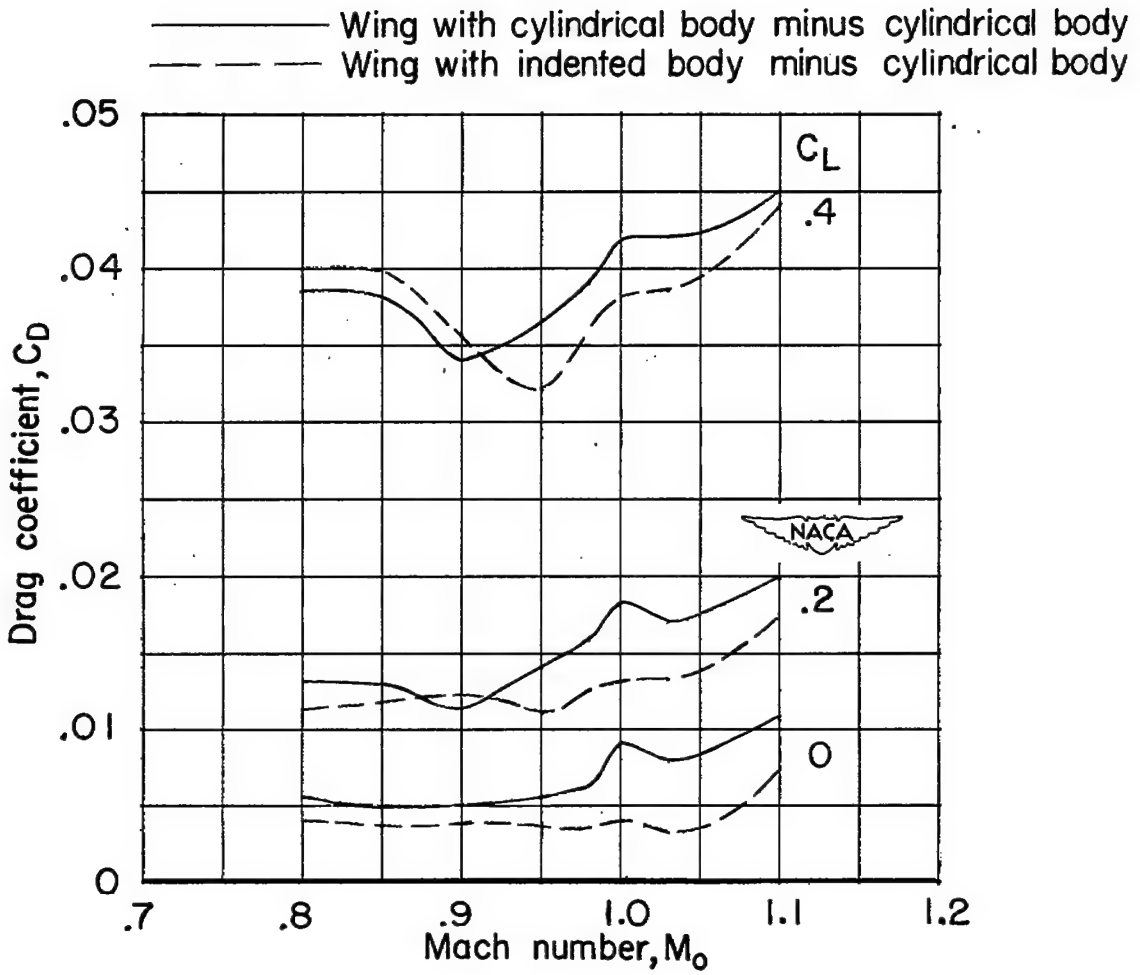

Figure 6.- Variation with Mach number of the wing with interference drag coefficient illustrating effect of body indentation on the transonic drag rise.

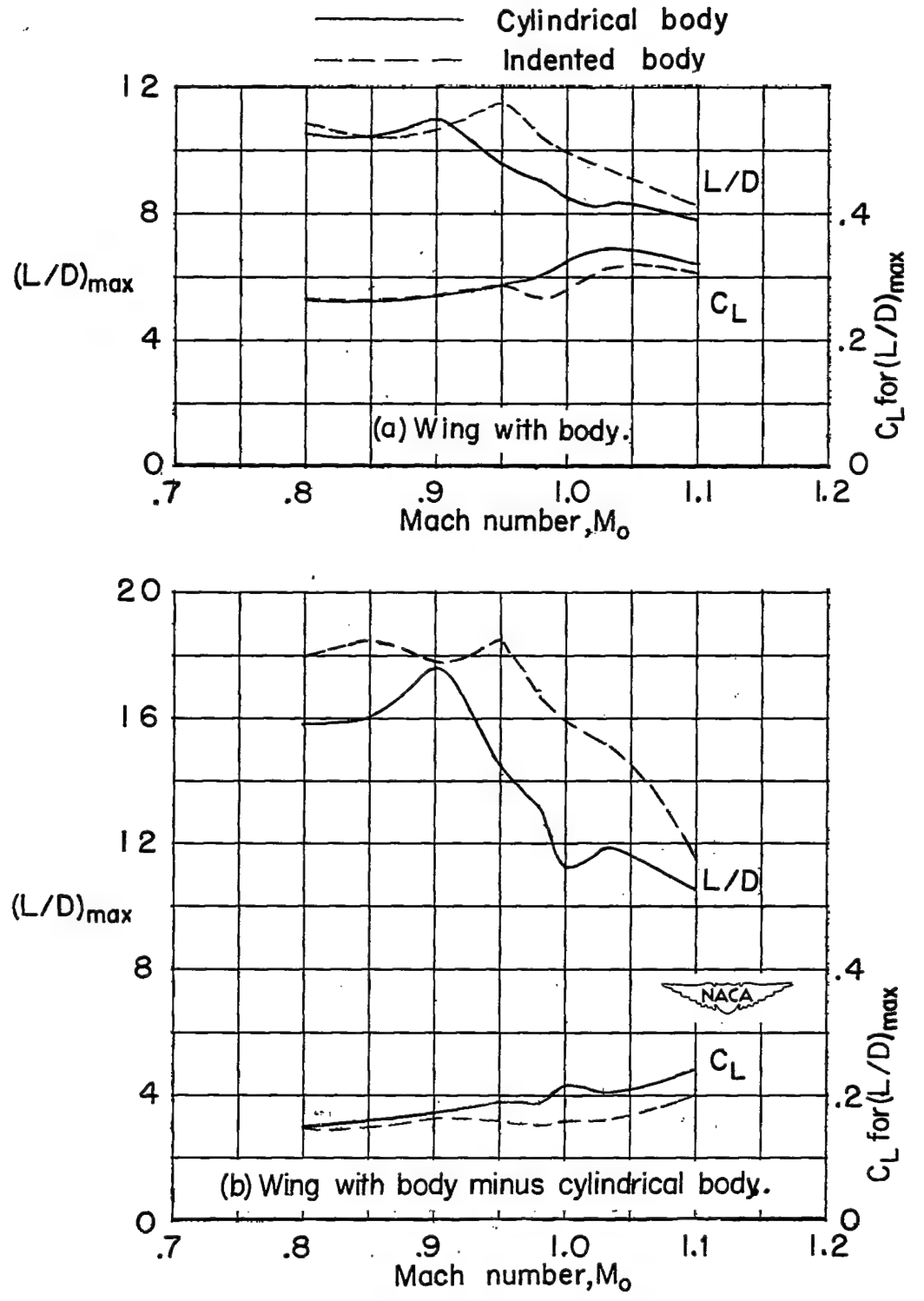

Figure 7.- Comparison of maximum lift-drag ratio and lift coefficient for maximum lift-drag ratio.

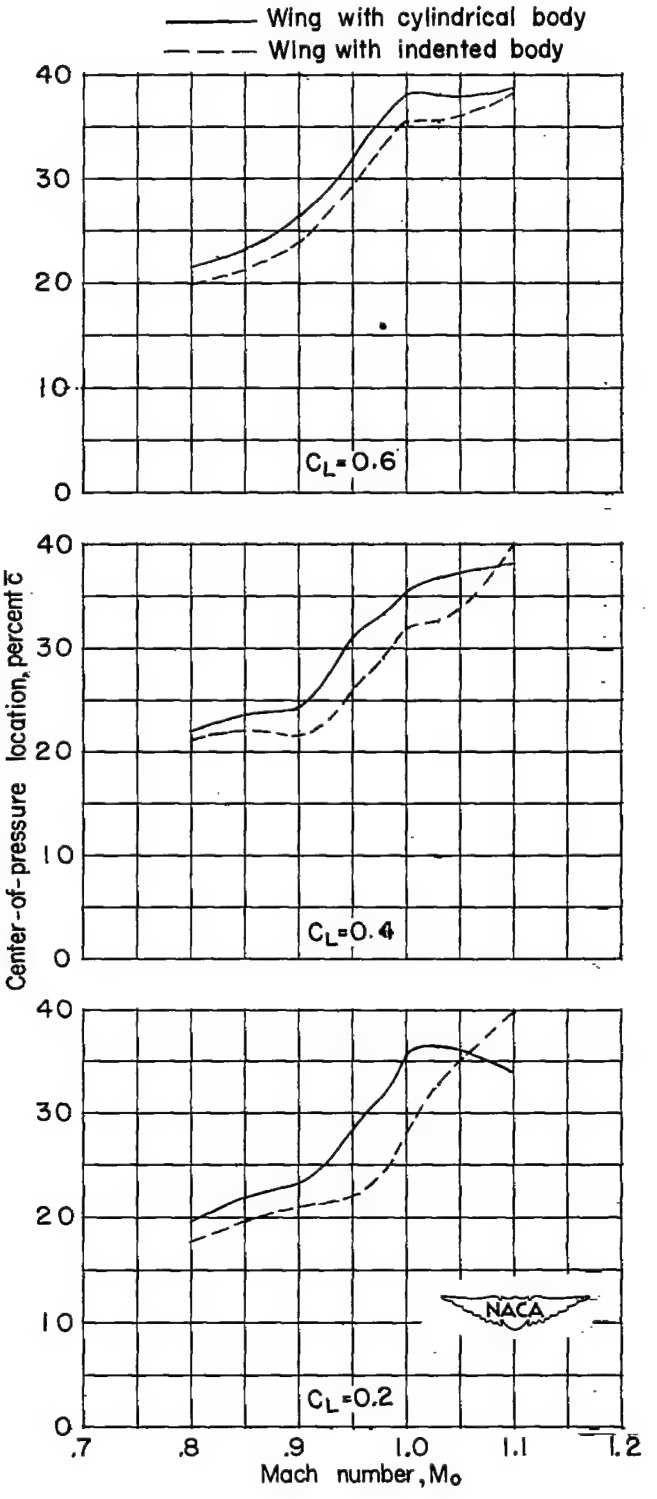

Figure 8.- Variation of center-of-pressure location with Mach number.

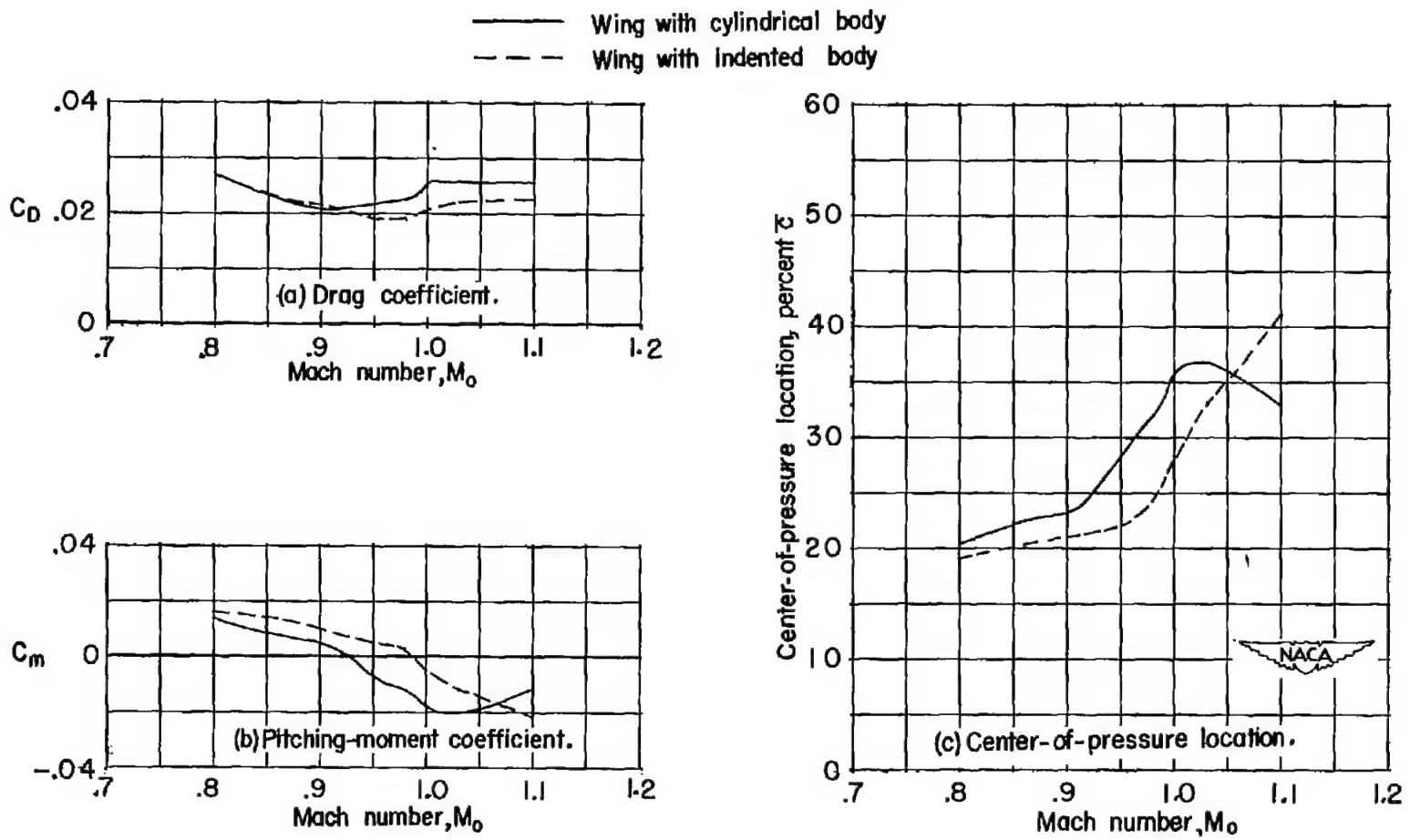

Figure 9.- Comparison of various performance parameters for level-flight condition at an altitude of 40,000 feet and a wing loading of 50 pounds per square foot.

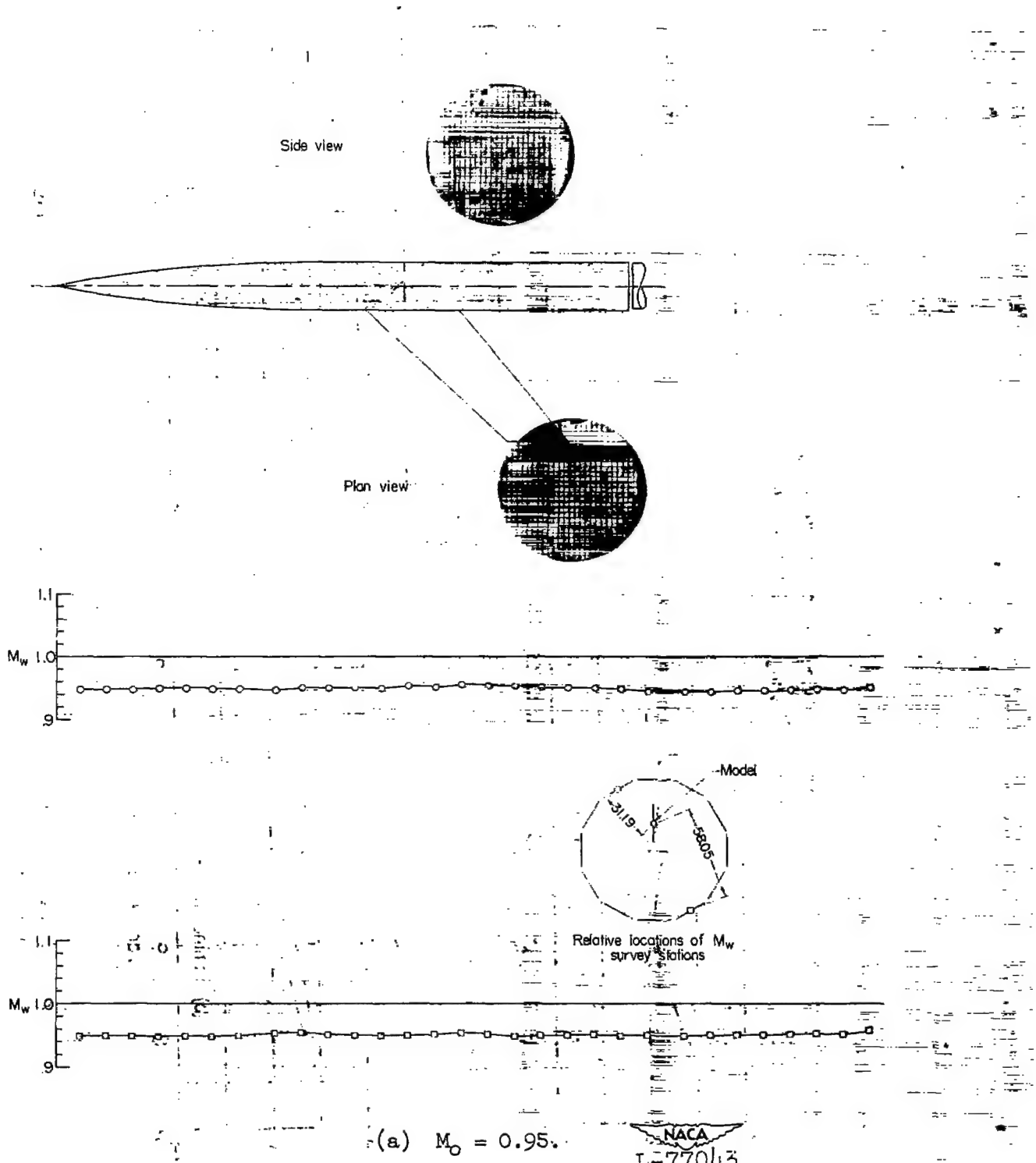

(a) $M_o = 0.95$.

Figure 10.- Shock phenomena for the zero lift case. All dimensions in inches.

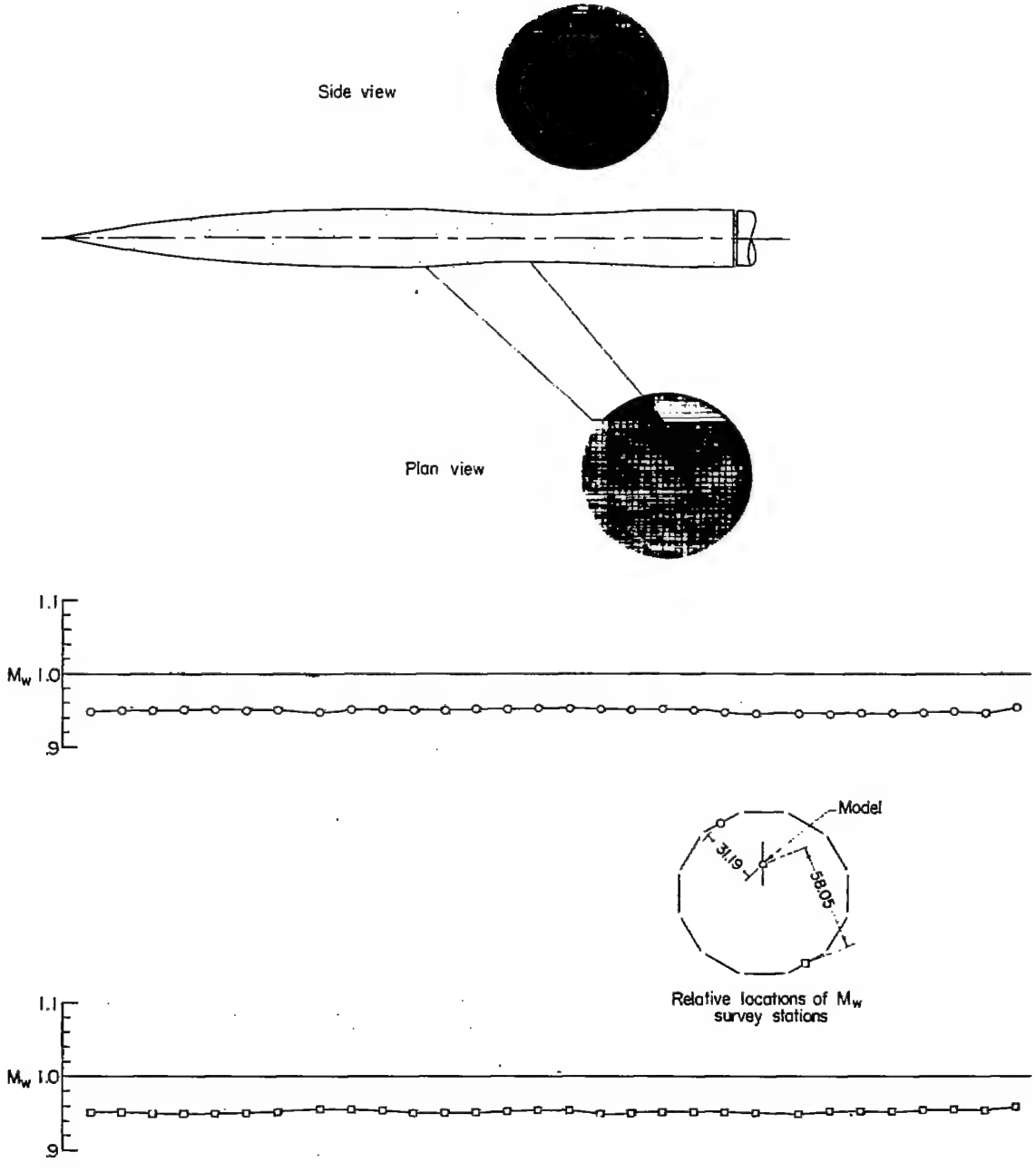

(a) M_O = 0.95. Concluded.

NACA L-77044

Figure 10.- Continued.

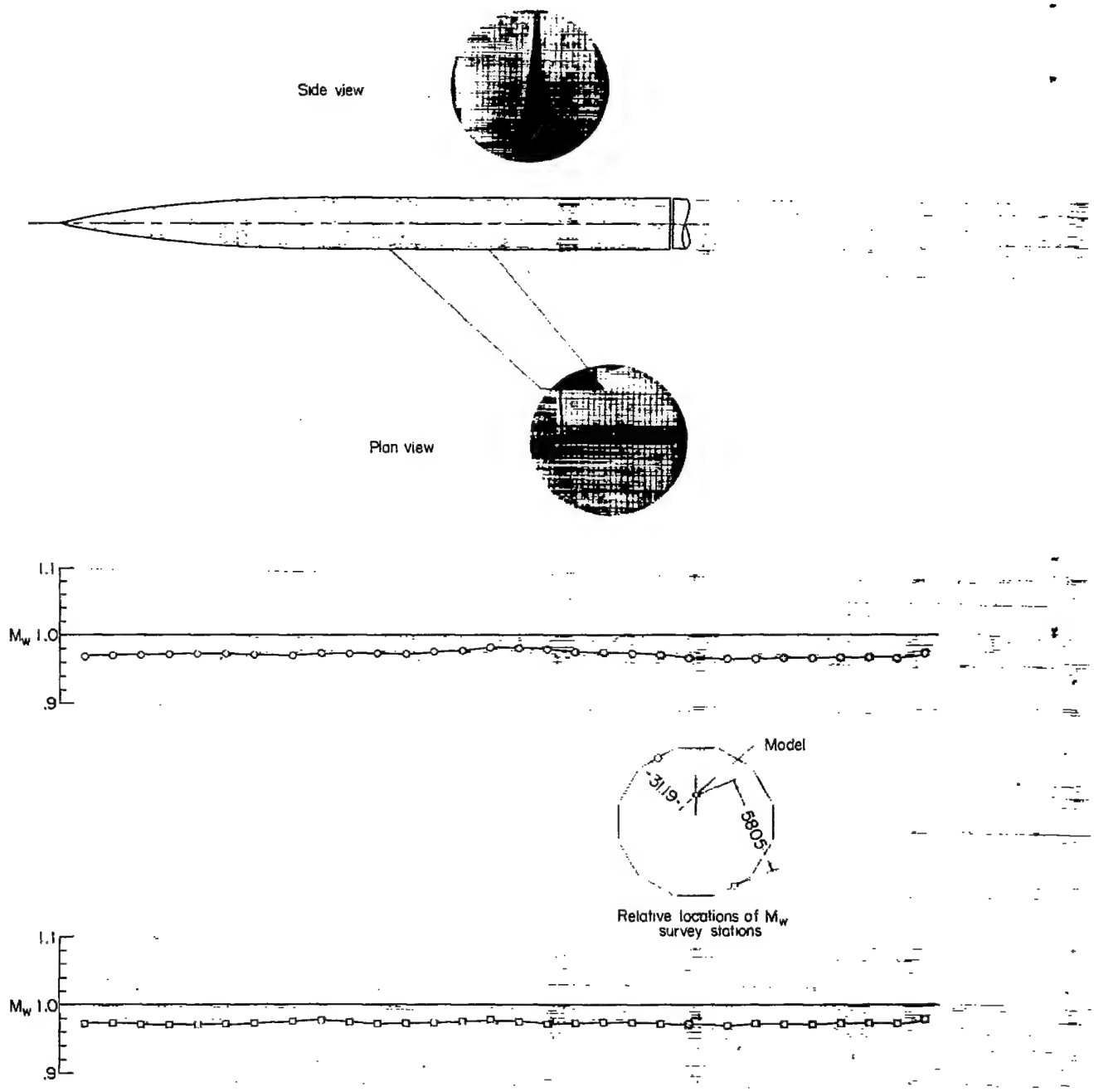

(b) M_o = 0.98.

NACA L-77045

Figure 10.- Continued.

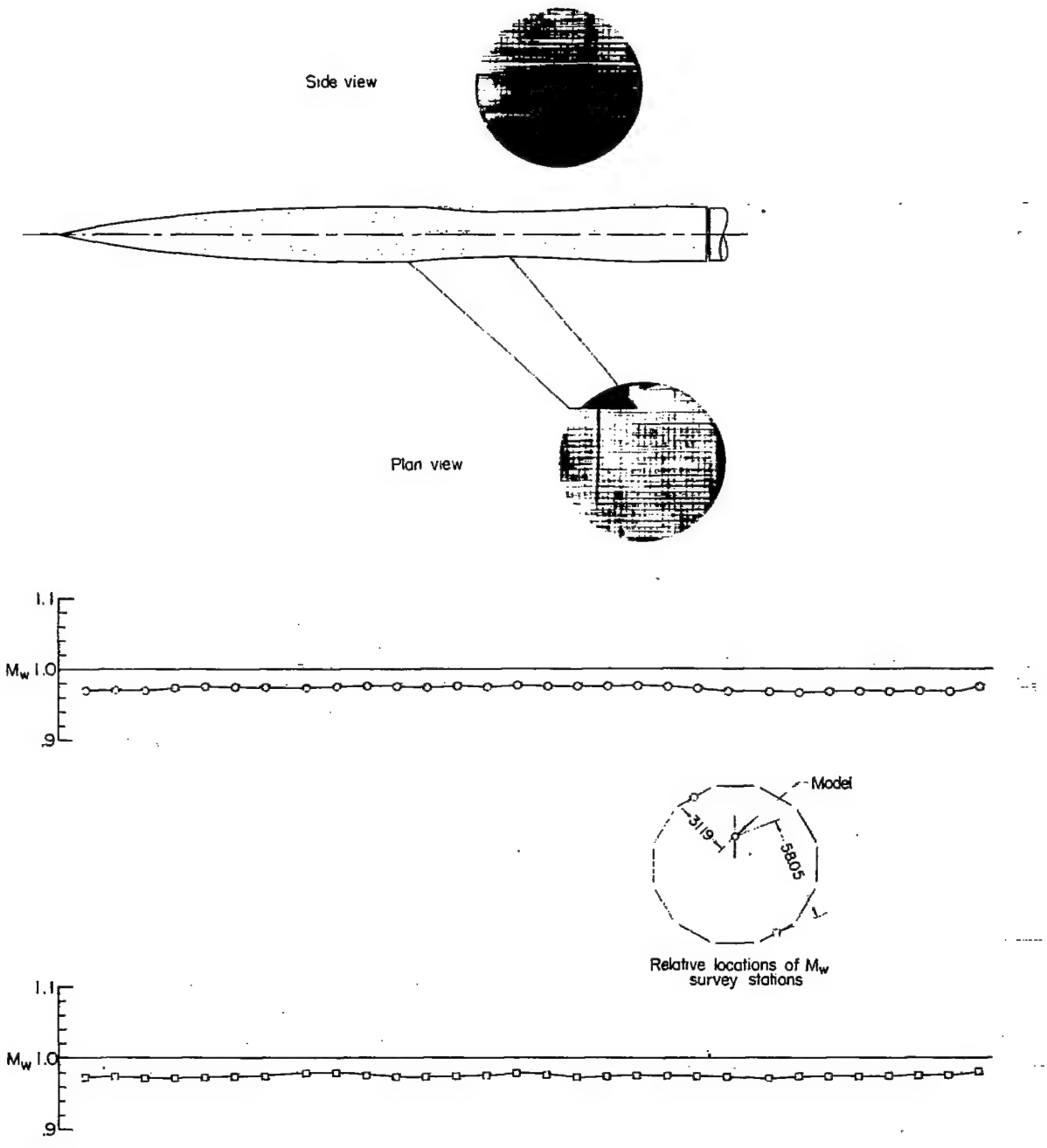

(b) M_o = 0.98. Concluded.

NACA L-77046

Figure 10.- Continued.

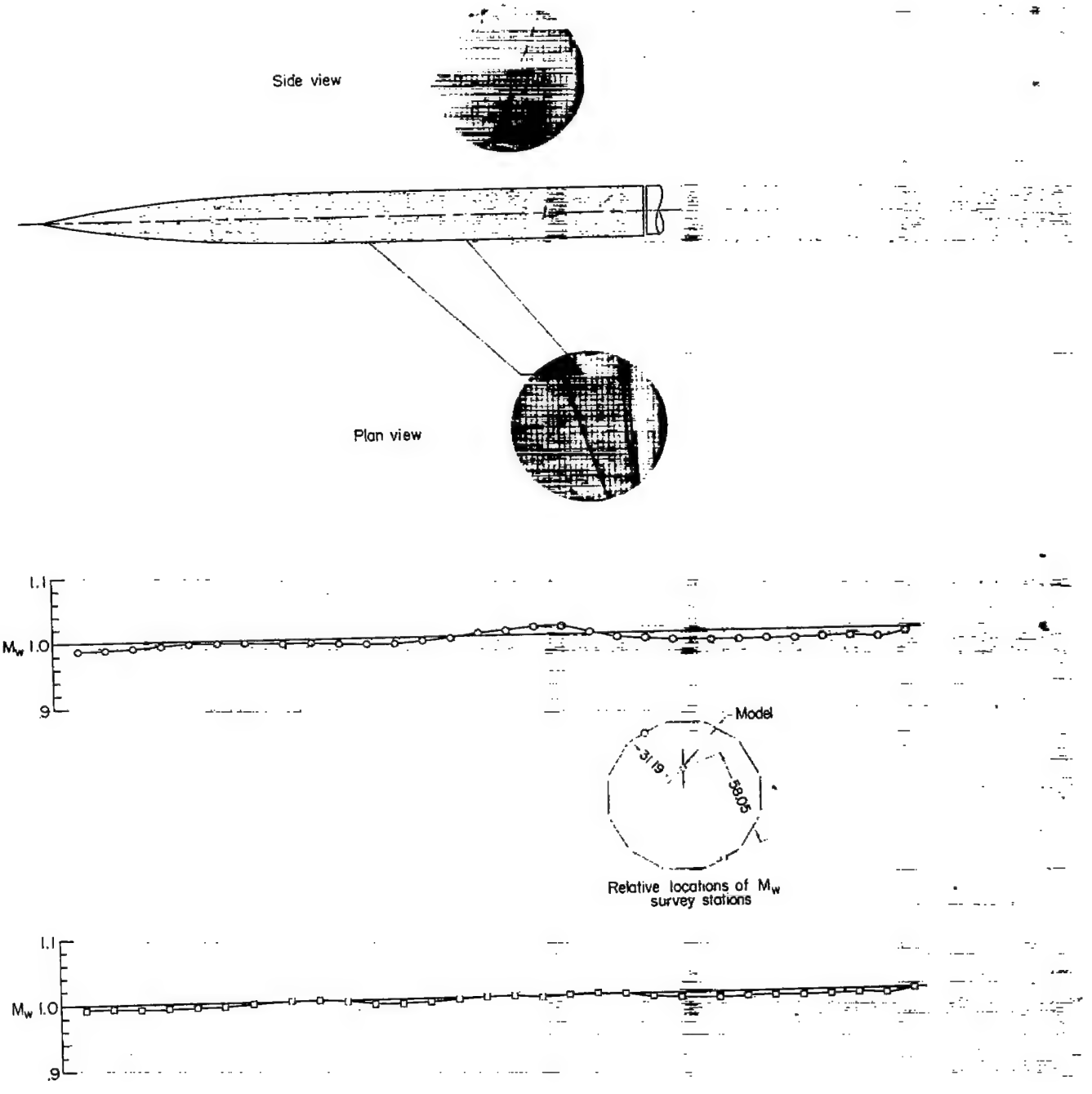

(c) M_o = 1.01.

NACA L-77047

Figure 10.- Continued.

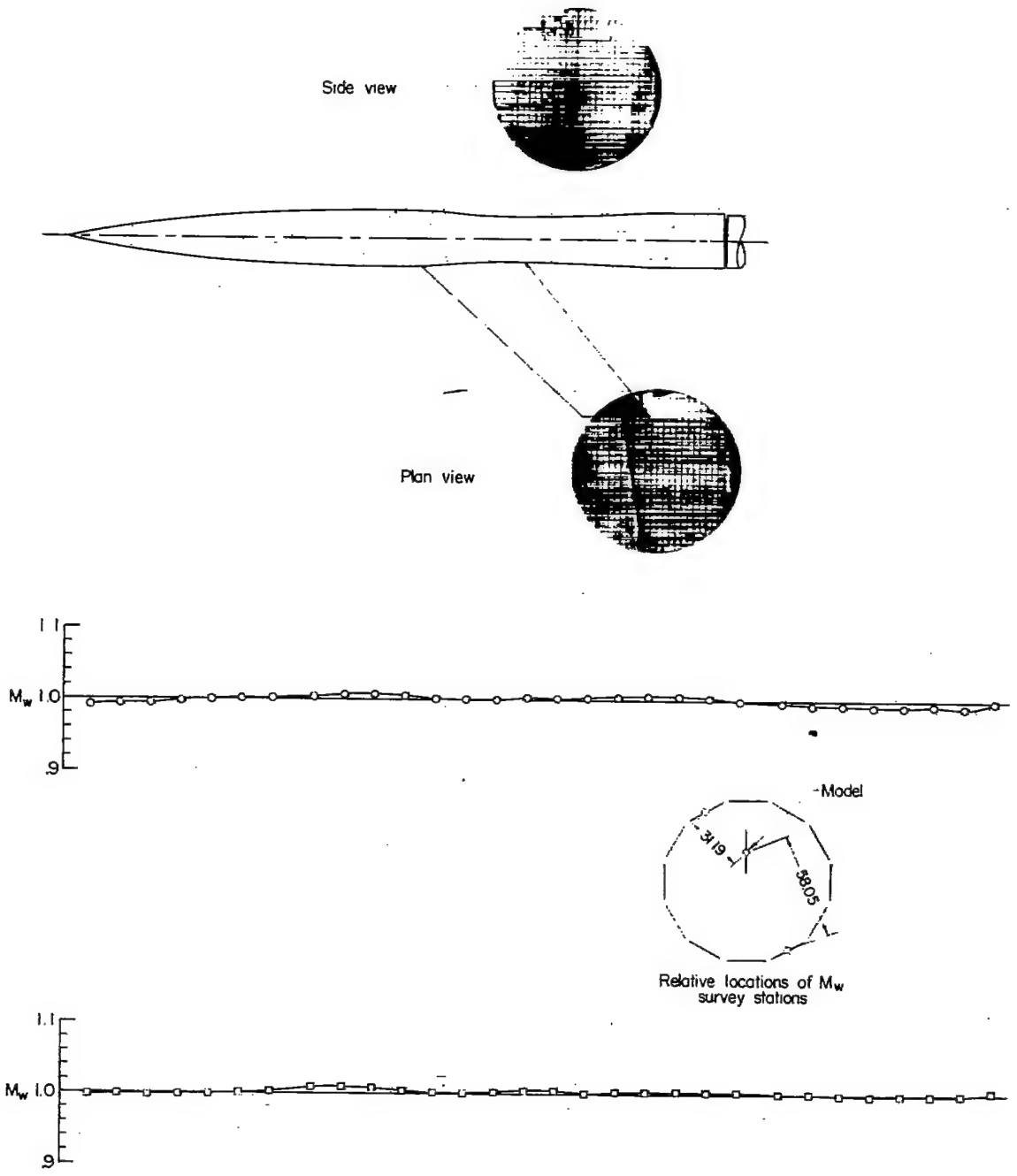

(c) M_o = 1.01. Concluded.

NACA L-77048

Figure 10.- Continued.

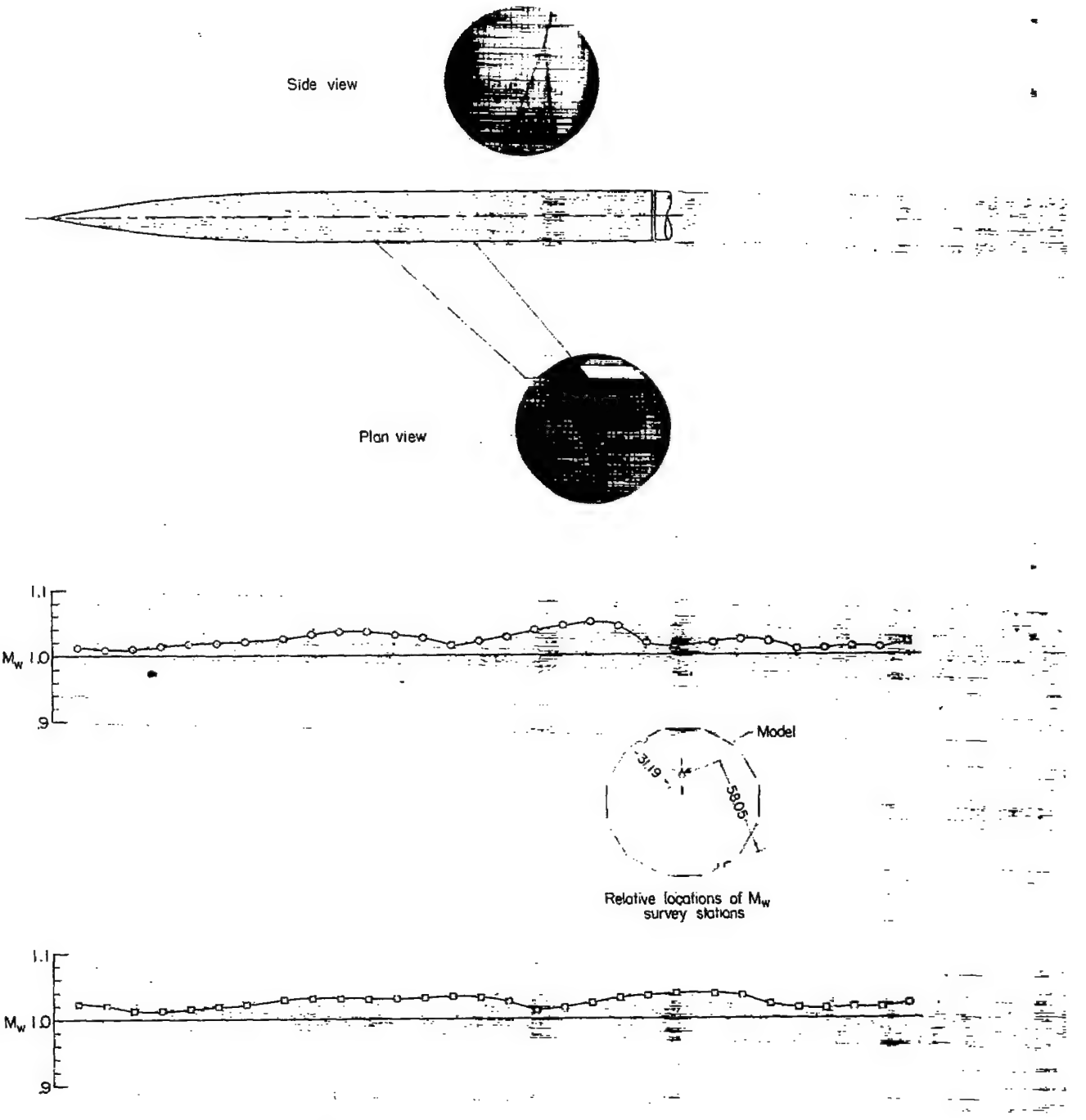

(d) M_o = 1.03.

NACA L-77049

Figure 10.- Continued.

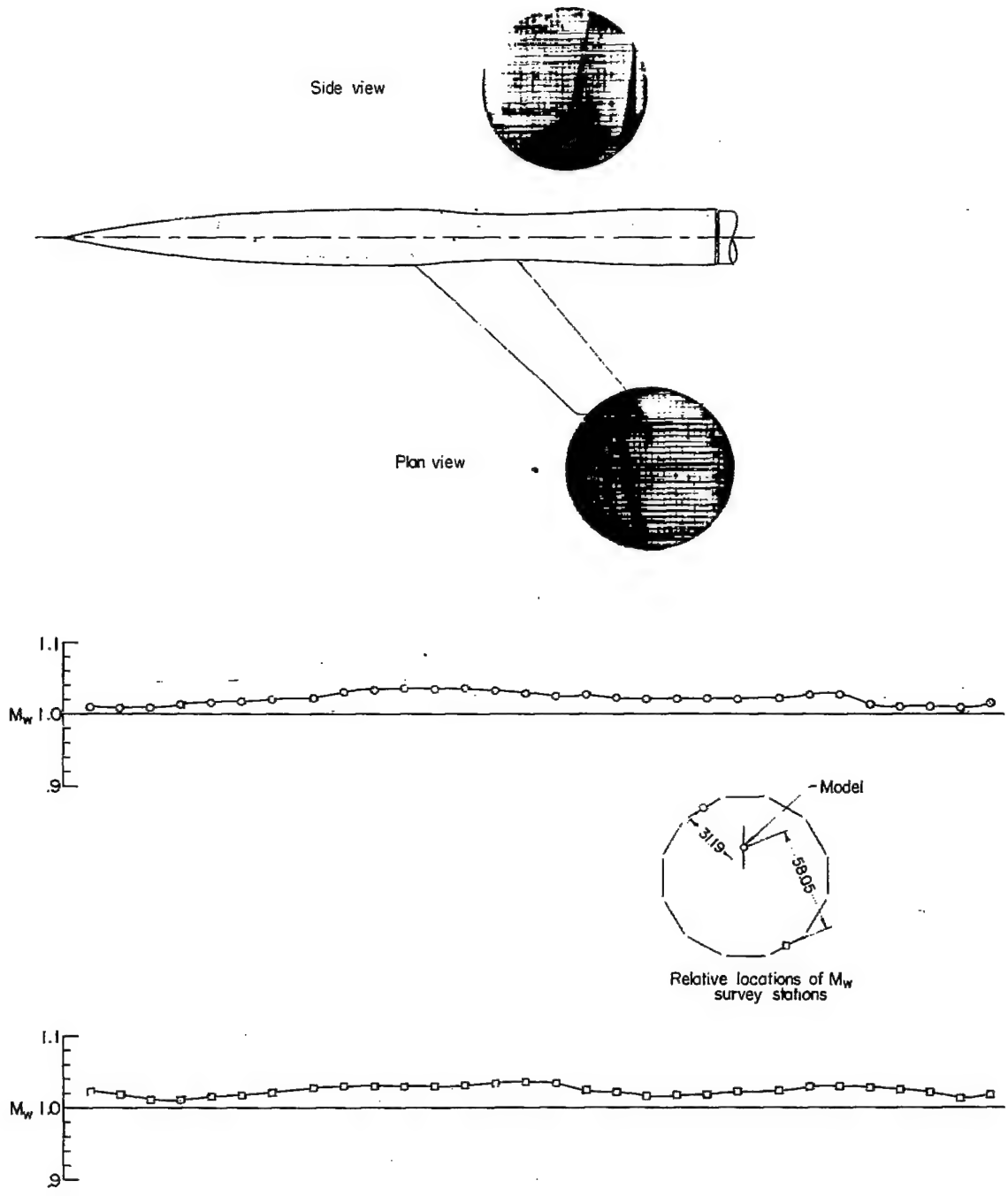

(d) M_o = 1.03. Concluded.

NACA L-77050

Figure 10.- Continued.

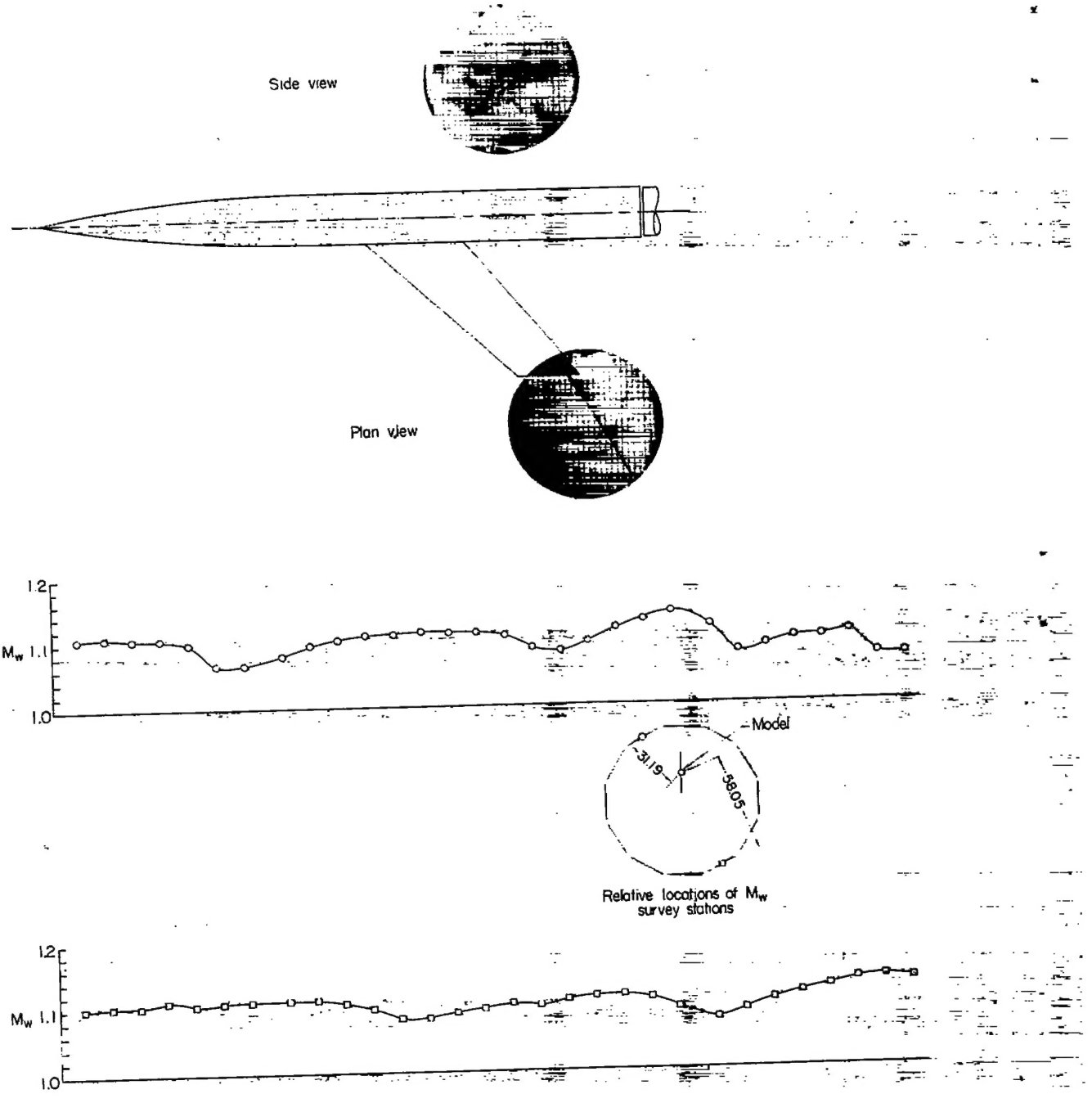

(e) $M_o = 1.11$.

NACA L-77869

Figure 10.- Continued.

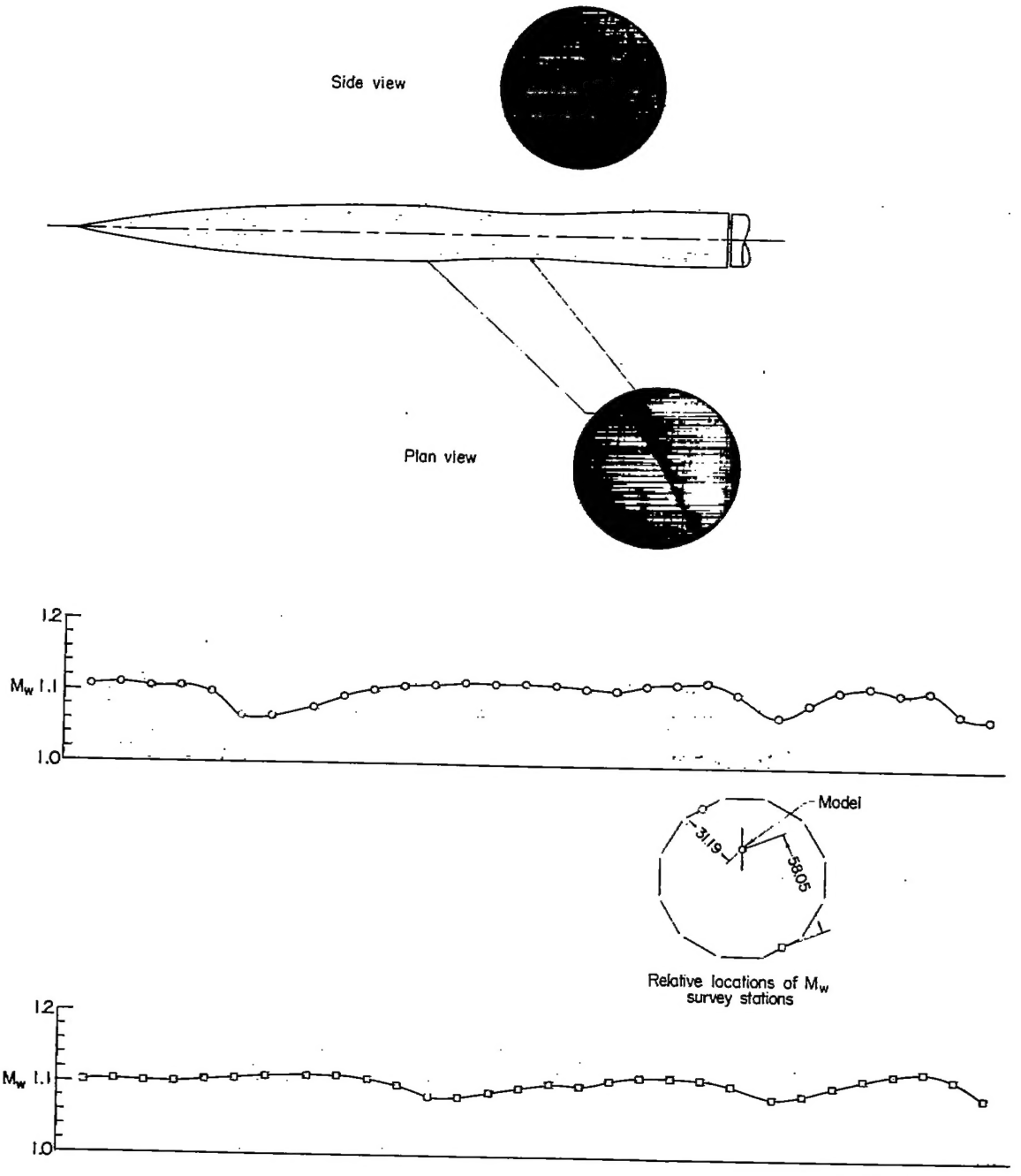

(e) M_o = 1.11. Concluded.

Figure 10.- Concluded.

NACA L-77870

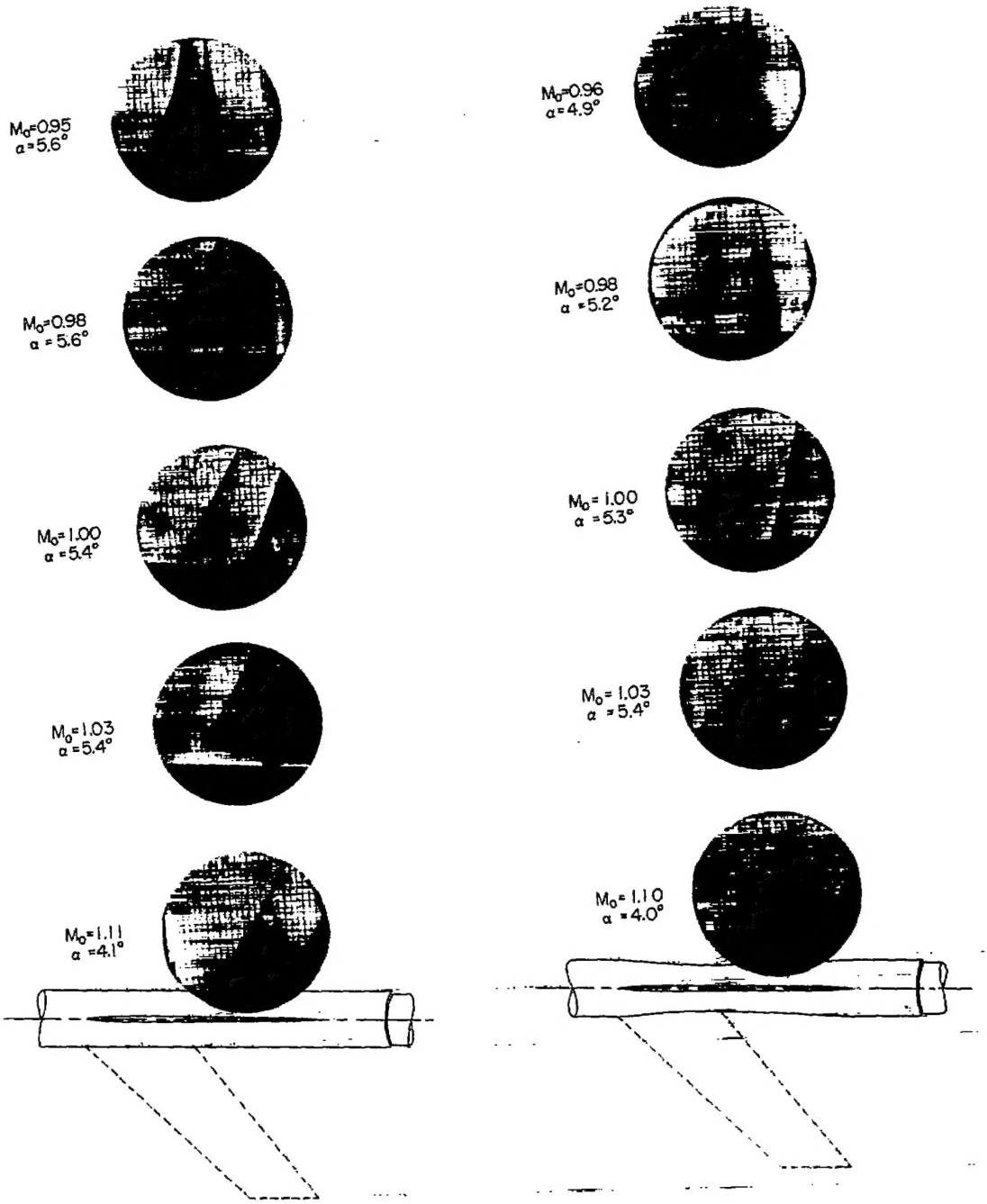

(a) Side view.

NACA L-77871

Figure 11.- Shock phenomena for the lifting case.

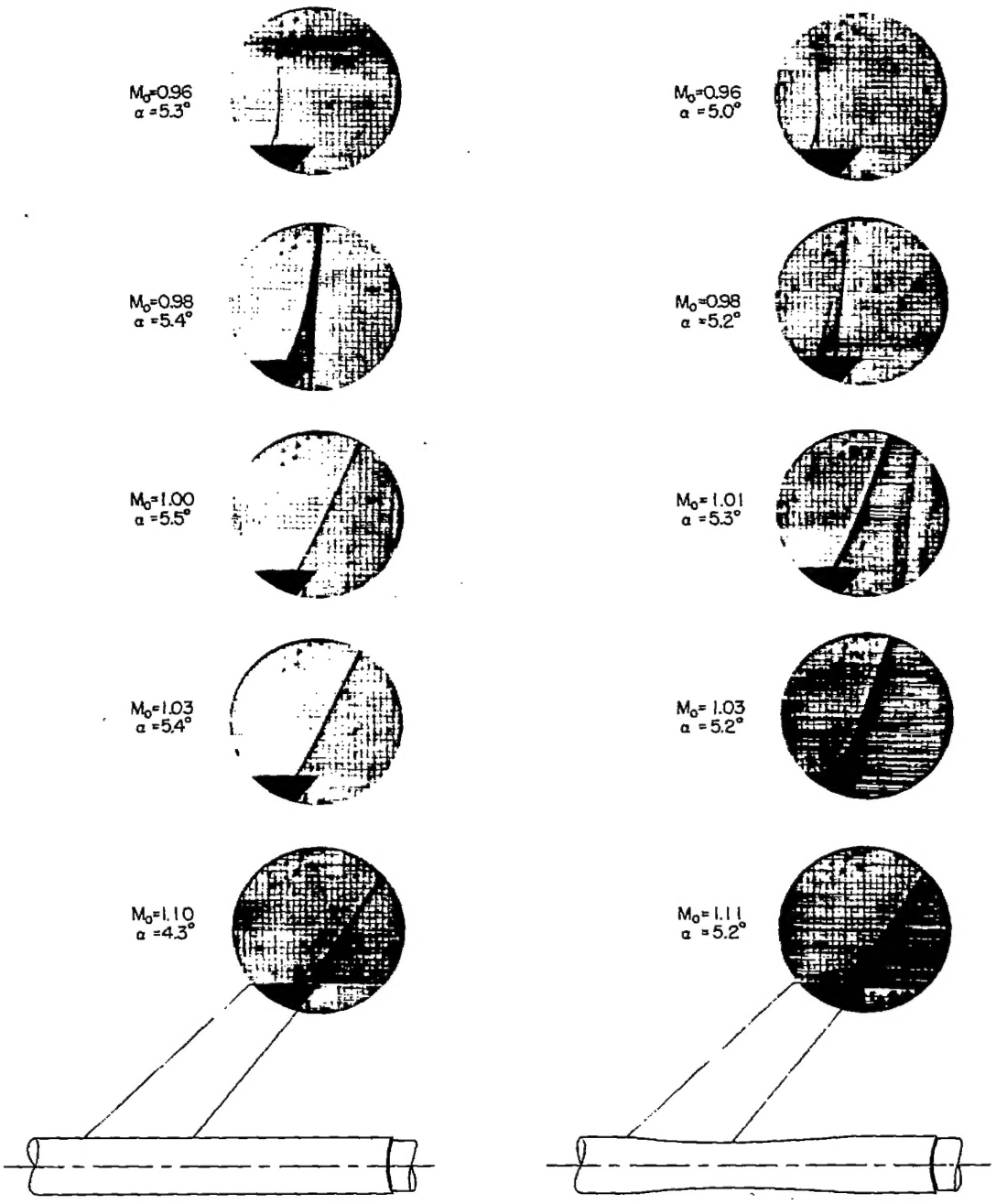

(b) Plan view.

NACA L-77872

Figure 11.- Concluded.

NACA-Langley - 2-9-53 - 325